

Assessment of the Upper Particle Size Limit for Quantitative Analysis of Aerosols Using Laser-Induced Breakdown Spectroscopy

Jorge E. Carranza and David W. Hahn*

Department of Mechanical Engineering, Box 116300, University of Florida, Gainesville, Florida 32611-6300

The laser-induced plasma vaporization of individual silica microspheres in an aerosolized air stream was investigated. The upper size limit for complete particle vaporization corresponds to a silica particle diameter of 2.1 μm for a laser pulse energy of 320 mJ, as determined by the deviation from a linear mass response of the silicon atomic emission signal. Comparison of the measured silica particle sampling rates and those predicted based on Poisson sampling statistics and the overall laser-induced plasma volume suggests that the primary mechanism of particle vaporization is related to direct plasma–particle interactions as opposed to a laser beam–particle interaction. Finally, temporal and spatial plasma evolution is discussed in concert with factors that may influence the vaporization dynamics of individual aerosol particles, such as thermophoretic forces and vapor expulsion.

Since the pioneering work of Radziemski and co-workers in the early 1980s, laser-induced breakdown spectroscopy (LIBS), also referred to as laser-induced plasma spectroscopy, has been widely used as an analytical technique for the quantitative analysis and monitoring of a wide range of aerosol particles.^{1–6} With recent increased interest in fine particulate matter, including effluent waste streams and ambient air aerosol loadings, researchers have focused efforts on the development of LIBS-based real-time monitoring techniques.^{7–12} Work by Hahn and co-workers has

focused on single-shot conditional analysis to improve the sensitivity of the LIBS technique for aerosol analysis by taking advantage of the discrete nature of aerosol particles and the subsequent LIBS response.¹³ As a consequence, this approach opened the door to the quantitative analysis of individual aerosol particles.^{14–16} Notwithstanding the significant body of research regarding laser-induced breakdown spectroscopy for aerosol analysis, to date no research has systematically addressed the fundamental assumption inherent in all quantitative LIBS measurements, namely, the assumption of complete breakdown and vaporization of all analyte species that comprise the aerosol particles of interest. The important question remains as to what is the upper particle size limit of complete dissociation and vaporization of individual particles suspended in a gas stream?

A survey of the literature regarding the largest particles that can be completely vaporized for quantitative LIBS-based analysis reveals no systematic study designed to specifically address this issue. Cremers and Radziemski¹⁷ explored LIBS for the detection of beryllium particles deposited on filters corresponding to particle diameters of 50 nm, an ensemble collection of particles ranging from 0.5 to 5 μm , and for nominally 15- μm -sized particles. They used a cylindrical lens to focus a laser beam directly on the surface of the filters, thereby producing a plasma that engulfed the deposited beryllium particles, and subsequently collected the spectral emission. Cremers and Radziemski reported a different analyte response, manifest as different calibration curve slopes, for these three different particle size classes, and concluded on the basis of their experimental observations that incomplete particle vaporization occurred for particles with diameters greater than $\sim 15 \mu\text{m}$. In other studies, Radziemski et al. explored direct LIBS-based analysis of beryllium aerosols using particles less than 10 μm in diameter,^{1,18} and noted in the latter study that such a particle size is consistent with complete particle vaporization. Several contemporary research papers have cited a 10- μm upper size limit for complete particle vaporization,^{2,5,13} some referring

* Corresponding author: (e-mail) dwhahn@ufl.edu; (phone) 352-392-0807; (fax) 352-392-1071.

- (1) Radziemski, L. J.; Loree, T. R.; Cremers, D. A.; Hoffman, N. M. *Anal. Chem.* **1983**, *55*, 1246–1252.
- (2) Ottesen, D. K.; Wang, J. C. F.; Radziemski, L. J. *Appl. Spectrosc.* **1989**, *43*, 967–976.
- (3) Ng, K. C.; Ayala, N. L.; Simeonsson, J. B.; Winefordner, J. D. *Anal. Chim. Acta* **1992**, *269*, 123–128.
- (4) Schechter, I. *Anal. Sci. Technol.* **1995**, *8*, 779–786.
- (5) Yalcin, S.; Crosley, D. R.; Smith, G. P.; Faris, G. W. *Hazard. Waste Hazard. Mater.* **1996**, *13*, 51–61.
- (6) Nunez, M. H.; Cavalli, P.; Petrucci, G.; Omenetto, N. *Appl. Spectrosc.* **2000**, *54*, 1805–1816.
- (7) Flower, W. L.; Peng, L. W.; Bonin, M. P.; French, N. B.; Johnsen, H. A.; Ottesen, D. K.; Renzi, R. F.; Westbrook, L. V. *Fuel Process. Technol.* **1994**, *39*, 277–284.
- (8) Neuhauser, R. E.; Panne, U.; Niessner, R.; Petrucci, G. A.; Cavalli, P.; Omenetto, N. *Anal. Chim. Acta* **1997**, *346*, 37–48.
- (9) Singh, J. P.; Yueh, F. Y.; Zhang, H. S.; Cook, R. L. *Process Control Qual.* **1997**, *10*, 247–258.
- (10) Neuhauser, N. E.; Panne, U.; Niessner, R.; Wilbring, P. *Fresenius J. Anal. Chem.* **1999**, *364*, 720–726.
- (11) Zhang, H.; Yueh, F. Y.; Singh, J. P. *Appl. Opt.* **1999**, *38*, 1459–1466.

- (12) Buckley, S. G.; Johnsen, H. A.; Hencken, K. R.; Hahn, D. W. *Waste Manage.* **2000**, *20*, 455–462.
- (13) Hahn, D. W.; Flower, W. L.; Hencken, K. R. *Appl. Spectrosc.* **1997**, *51*, 1836–1844.
- (14) Hahn, D. W. *Appl. Phys. Lett.* **1998**, *72*, 2960–2962.
- (15) Hahn, D. W.; Lunden, M. M. *Aerosol Sci. Technol.* **2000**, *33*, 30–48.
- (16) Carranza, J. E.; Fisher, B. T.; Yoder, G. D.; Hahn, D. W. *Spectrochim. Acta Part B* **2001**, *56*, 851–864.
- (17) Cremers, D. A.; Radziemski, L. J. *Appl. Spectrosc.* **1985**, *39*, 57–63.
- (18) Essien, M.; Radziemski, L. J.; Sneddon, J. J. *Anal. At. Spectrom.* **1988**, *3*, 985–988.

to the extensive work of Radziemski and Cremers and some not citing any particular reference source. Based on the overall body of LIBS research, it appears that what was presented by Radziemski et al. as a useful guideline for quantitative LIBS analysis of aerosols, namely, the 10- μm upper size limit, has in essence become the accepted upper size limit for complete vaporization of aerosol particles within laser-induced plasmas. However, to the best of our knowledge, no research has been reported that specifically addresses the issue of complete vaporization of individual airborne particles using laser-induced breakdown spectroscopy. The present paper attempts to address this critical need regarding the upper size limit for complete vaporization of individual aerosol particles with the LIBS technique.

EXPERIMENTAL SYSTEM AND METHODOLOGY

The LIBS experimental setup and the aerosol generation system were presented in a previous paper,¹⁹ and only a short description concerning the present study is given here. A 1064-nm Q-switched Nd:YAG laser operating with 320-mJ pulse energy, 10-ns pulse width, and 5-Hz pulse repetition rate was used as the plasma source. The laser pulse energy corresponds to the saturation region with respect to laser pulse energy absorption by the plasma, as reported recently for the current optical system.²⁰ The saturation regime is characterized by a higher precision with respect to atomic emission characteristics (e.g., peak-to-base ratios). To create the plasma, an expanded laser beam 12 mm in diameter was focused to a beam spot of 100- μm diameter inside the aerosol sample chamber using a 75-mm UV grade plano-convex lens. The plasma emission was collected along the incident beam in a backward direction and separated using a 50-mm elliptical pierced mirror. The collected light was launched into an optical fiber bundle coupled to spectrometer (2400 groove/mm grating, 0.12-nm optical resolution) and recorded with an intensified charge-coupled device (iCCD) array.

Aerosols were generated by the nebulization of aqueous solutions of silicon (ICP-grade silicon standards) and of monodisperse silica particle suspensions (spherical SiO_2 particles with monodisperse diameters ranging from 1.0 to 5.1 μm) in deionized water. The nebulizer used 5 L/min dry nitrogen, and the nebulizer output was subsequently mixed with a gaseous coflow stream of 42 L/min purified, dry air. For the case of the aqueous silicon solutions, well-dispersed nanoparticles were produced in the LIBS aerosol sample chamber following droplet evaporation, with a mean particle size of ~ 50 nm, as verified using TEM analysis, and corresponding particle number density on the order of 10^7 cm^{-3} .¹⁹ For the case of the monodisperse silica particle suspensions, the particle concentrations in solution were adjusted (using ultrapurified water dilution) to produce aerosol particle number densities of ~ 45 cm^{-3} in the LIBS sample chamber, as based on the nebulization rate of the liquid suspension, known particle concentration in suspension, and known total gas flow rates. The particle concentrations in suspension were calculated based on serial dilution of the original particle suspensions as supplied by the manufacturer and were verified using laser transmission measurements in combination with calculated Mie extinction coefficients. All particle suspensions were subjected to sonication

before and periodically throughout all experiments to reduce potential particle agglomeration.

LIBS-based analysis for all experiments used the neutral silicon atomic emission line at 288.16 nm. The processed LIBS signal was the ratio of the integrated atomic emission line peak area to the continuum base emission intensity, referred to as the peak-to-base (P/B) ratio. The continuum intensity was interpolated by using the adjacent, featureless continuum emission intensity on both sides of the silicon emission line. For temporal signal integration, the 288.16-nm Si I emission line intensity (peak-to-base ratio) was optimized using a 35- μs time delay with respect to the incident laser pulse and an integration time of 5 μs . Ensemble averaging (minimum of 3000 individual spectra at each known aqueous silicon concentration) was used to construct a linear calibration response curve of the 288.16-nm silicon P/B signal as a function of known silicon mass concentration in the LIBS sample chamber. The calibration curve was constructed using the aqueous silicon standard solutions; hence, the response was constructed for a well-dispersed aerosol flow of silicon nanoparticles that corresponded to the order of 10^4 particles per plasma volume.

Single-shot conditional analysis was used to identify and analyze individual spectra corresponding to the various sized monodisperse silica particles. The conditional data analysis routine was reported previously^{13,15} and entails the identification of individual LIBS spectra corresponding to the presence of discrete particles within a given plasma volume based on the targeted analyte atomic emission signal exceeding a predetermined threshold value. For the current study, the threshold value for the 288.16-nm silicon emission peak was set to obtain an average of 3 false hits (i.e., hits recorded for the nebulization of purified water) for every 1000 laser shots for nearly all experiments. To assess the effect of the threshold value, additional experiments were performed for analysis of the 1.0- μm silica particles using a more relaxed threshold value such that ~ 30 false hits were recorded for each 1000 shots. For all spectral data processing, individual spectra were smoothed using the Savitzky–Golay algorithm^{21,22} and subsequently processed using the 288.16-nm silicon emission line profile as follows.

After all single-shot spectra were smoothed, a spectral filtering algorithm was used to screen out false hits and any other anomalous spectra (such as aerosol breakdown outside of the primary plasma volume) resulting from the discrete sampling of aerosol particles. As noted above, the conditional analysis threshold value was set to allow the detection of a small number of false hits, that is, spectra that contain no actual silicon emission. This was accomplished by setting the threshold in a purified air stream with the nebulization of only ultrapurified water. The presence of a small number of false hits ensures that the single-shot detection threshold is sufficiently low to enable identification of actual analyte hits at signal levels approaching the upper single-shot noise limit realized for a given spectral location. The false hits were subsequently filtered out using the following approach. The filtering algorithm is based on the similarity of the silicon emission line profile for a given single-shot spectrum as compared to emission line profile corresponding to the ensemble average of

(19) Hahn, D. W.; Carranza, J. E.; Arsenault, G. R.; Johnsen, H. A.; Hencken, K. *Rev. Sci. Instrum.* **2001**, *72*, 3706–3713.

(20) Carranza, J. E.; Hahn, D. W. *Spectrochim. Acta Part B* **2002**, *57*, 779–790.

(21) Savitzky A.; Golay, M. J. E. *Anal. Chem.* **1964**, *36*, 1627–1639.

(22) Madden, H. H. *Anal. Chem.* **1978**, *50*, 1383–1386.

thousands of individual spectra recorded for the aqueous silicon standard solutions as discussed above. Specifically, the silicon line profile of a given single-shot spectrum was compared to the "standard" line profile using a width of 12 pixels, which corresponds to the full-width (90%) of the silicon emission line. Accepted spectra deviated from the template profile by less than 7–30% over the full width half-maximum and by less than 60–90% over the remaining line width. These specified percent deviations were decreased approximately linearly over the line profile for each range (i.e., 7–30 and 60–90%). This filtering algorithm resulted in the rejection of ~60% of all identified particle "hits", for the trigger threshold corresponding to an average of 3 false hits (i.e., no silicon present) per 1000 shots. More importantly, the spectral rejection rate was consistent over all particle sizes. Additional experiments were combined with an alternative data processing scheme based on a comparison of the silicon line signal-to-noise ratio (SNR) with the SNR of an adjacent, continuum spectral region to corroborate the above algorithm and results using the 2.1- μm -sized microspheres. Analysis of the ensemble average of all identified and accepted silica particle hits yielded an equivalent particle mass in excellent agreement with the known 2.1- μm silica particle mass, while the spectral data rejection rates were consistent with the rate observed for the present algorithm.

When the relaxed conditional analysis threshold criteria was used, namely, 30 false hits per 1000 shots, the data rejection rate scaled exactly with the 10-fold increase in false particle hits, thereby demonstrating the independence of the final data set on the exact threshold value used for hit detection. Overall, the spectral data processing results were in excellent agreement with the expected outcome based on the estimated silica particle loadings, plasma volume sampling rates, and conditional sampling threshold values.

RESULTS AND DISCUSSION

The first set of experiments was designed to quantify the response of the 288.16-nm silicon line for a range of known silicon mass concentrations, with silicon present as the finely dispersed nanoparticles generated by nebulization of the aqueous silicon standard solutions. It is noted that for, the plasma volume realized in the present study (measured as an ~ 1.5 mm equivalent spherical diameter), there were on the order of 10^4 silicon nanoparticles per plasma volume. As such, the resulting data represent the idealized LIBS-based analyte response corresponding to a highly homogeneous aerosol gas stream. The resulting silicon calibration curve was characterized by a linear correlation ($R > 0.999$) between the 288.16-nm silicon emission signal (P/B) and the known silicon mass concentration over the range from 0 to 17 300 $\mu\text{g}/\text{m}^3$. The high degree of linearity over the full range of silicon concentrations confirms the absence of self-absorption for concentrations as high as 17 300 $\mu\text{g}/\text{m}^3$, or ~ 14.9 parts per million on a mass basis. This upper limit was the highest concentration investigated (corresponding to the most concentrated standard silicon aqueous solution used for this study) and does not imply the onset of self-absorption above this value.

To investigate the upper size limit for complete particle vaporization, single-shot spectra corresponding to individual silica particles were collected and quantitatively analyzed for a range of the monodisperse silica particle diameters. It is noted that single-shot LIBS spectra display considerable spectral noise as

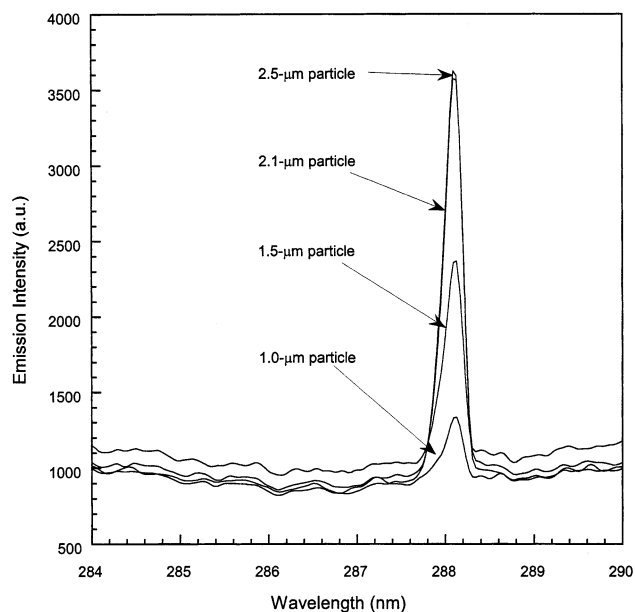


Figure 1. Ensemble-averaged spectra corresponding to individually detected monodisperse silica microspheres with diameters of 1.0, 1.5, 2.1, and 2.5 μm .

compared to ensemble-averaged spectra; hence, it is desirable to improve the SNR for quantitative analysis of spectra corresponding to the relatively small silica microspheres. Therefore, the Savitzky–Golay smoothing algorithm was used to suppress the level of random shot noise for each spectrum identified as corresponding to a silicon particle "hit" using the conditional analysis routine. This algorithm was demonstrated to have a negligible effect on the LIBS analyte signal (less than 1% change in the silicon emission line P/B ratio) as applied by utilizing a filter template width greater than the line width of the targeted atomic emission peak.

Single-shot spectra were recorded for each of the monodisperse silica particle suspensions, namely, for particle diameters equal to 1.0, 1.5, 2.1, 2.5, 3.0, 4.5, and 5.1 μm . Using the spectral data processing schemes outlined above, all single-shot spectra were processed and a final ensemble-averaged spectrum was calculated for each silica particle size composed of the individual single-shot spectra accepted after all data filtering. Representative ensemble-averaged spectra for the 1.0-, 1.5-, 2.1-, and 2.5- μm -diameter silica microspheres are shown in Figure 1. Last, the P/B of the 288.16-nm silicon line was calculated for each final ensemble-averaged spectrum. In Figure 2, the corresponding P/B for the different silica particle sizes are plotted as a function of the cube of the silica particle diameter, noting that the cubed diameter is proportional to the particle silicon mass. The most significant result of the Figure 2 data is the clearly linear relation between the silicon P/B ratio as a function of diameter cubed for the smallest three silica particle diameters (1.0, 1.5, and 2.1 μm) and the abrupt deviation from this linear trend for the particle diameters larger than 2.1 μm . For complete silica particle dissociation and vaporization, the resulting analyte signal (i.e., P/B) should scale as the analyte mass contained in the particle, hence as the diameter cubed. Accordingly, the break point in the Figure 2 data represents the upper size limit in which an aerosolized silica particle is completely vaporized in the laser-induced plasma. The

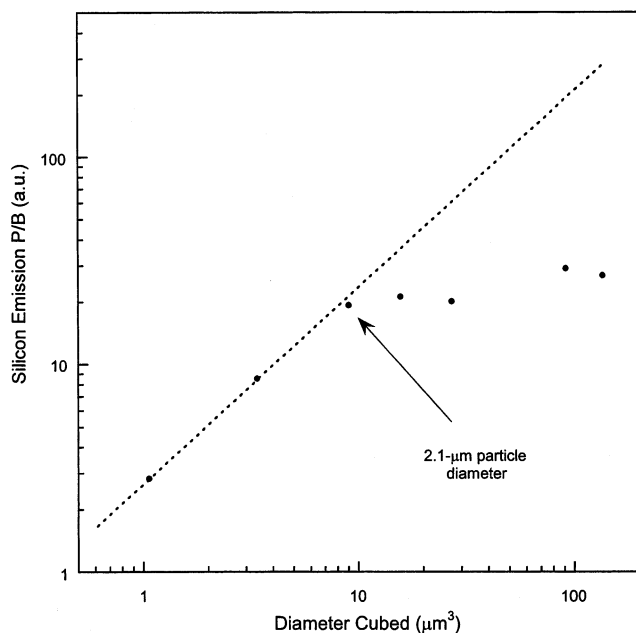


Figure 2. Peak-to-base (P/B) ratio of the 288.16-nm silicon atomic emission line for ensemble-averaged spectra of individually detected monodisperse silica microspheres as a function of the cube of the silica particle diameter. The dashed line is a linear fit of the first three data points.

limiting particle size of $2.1 \mu\text{m}$ is significantly below the frequently used $10\text{-}\mu\text{m}$ particle diameter limit and should be taken into consideration for LIBS-based analysis of aerosol systems.

In view of the well-defined upper size limit observed for the current study of silica particles, it is useful to discuss two fundamental phenomena that may play key roles in the dissociation and vaporization of the single aerosol particle, namely, laser-particle interactions and plasma-particle interactions. The first step in understanding the possible mechanisms responsible for an upper size particle limit is determining the relative importance of particle vaporization as a result of direct interaction with the incident laser pulse (i.e., laser-particle interaction) as compared to particle vaporization within the laser-induced plasma after the incident laser pulse (i.e., plasma-particle interaction). Careful examination of the silica particle sampling rates was performed to further elucidate the contributions of these two effects. For the present experiments, the laser beam was focused to a spot size measured as $\sim 100 \mu\text{m}$ in diameter. The resulting laser-induced plasma had a volume corresponding to an equivalent spherical diameter of $\sim 1.5 \text{ mm}$, as directly measured using transmission of a 532-nm probe beam synchronized to the tail end of the plasma-generating laser pulse. For sampling of discrete aerosol particles, the probability of a particle being in a specified sample volume (either the spatial region defined by the laser beam or the spatial region defined by the entire plasma volume) can be modeled by a Poisson probability distribution^{13,15} based on the respective sample volume and the aerosol number density. For the silica microsphere suspensions, LIBS-based particle sampling rates were predicted based on either the laser beam sample volume or the plasma sample volume. The predicted particle sample rates based on the plasma sample volume were in excellent agreement when compared to the actual experimental silica particle sampling rates (7 and 4%, respectively). In contrast, the predicted sample rates

based on the more limiting laser beam sample volume underpredicted the observed sample rate by 2 orders of magnitude. Based on this assessment, particle vaporization via direct laser-particle interaction can only account for less than 1% of the sampled silica particles actually measured; hence, the current experiments support the conclusion that plasma-particle interactions drive the dissociation and vaporization of individual aerosol particles. With this concept of plasma-particle interaction in mind, it is useful to examine the vaporized particle mass as compared to the plasma parameters and in consideration of the overall range of linear analyte response as reported above.

Spectral analysis of the LIBS signal corresponding to the upper size limit for complete vaporization ($2.1\text{-}\mu\text{m}$ SiO_2 particle) produced a silicon P/B signal corresponding to an equivalent concentration of $1925 \mu\text{g}/\text{m}^3$, as based on the linear calibration curve. In contrast, the $2.5\text{-}\mu\text{m}$ -sized silica particles, the smallest size examined that is characterized by incomplete vaporization, yielded an equivalent concentration of $2116 \mu\text{g}/\text{m}^3$ based on the silicon emission signal. This value is significantly less than the equivalent concentration of $\sim 3340 \mu\text{g}/\text{m}^3$ expected for a linear analyte response corresponding to complete vaporization of a $2.5\text{-}\mu\text{m}$ silica particle. It is noted that the calibration curve based on the high aerosol number density of silicon nanoparticles ($\sim 10^4$ particle per plasma) yielded a linear silicon analyte response to concentrations of at least $17\,300 \mu\text{g}/\text{m}^3$. A silicon mass concentration of $17\,300 \mu\text{g}/\text{m}^3$ corresponds to more than 5 times the silicon mass within a given plasma volume as compared to the mass produced by vaporization of a single $2.5\text{-}\mu\text{m}$ -sized silica particle. This behavior is somewhat surprising and provides strong evidence that the limiting factor for complete particle vaporization is not simply the total heat capacity of the plasma or the total analyte mass contained within the plasma volume. In fact, it is estimated that complete dissociation and vaporization of a single $2.5\text{-}\mu\text{m}$ silica particle would consume on the order of 0.0003% of the total plasma energy, as based on the combination of the heats of fusion and vaporization of silica as well as the sensible heat. These results suggest that the plasma-particle vaporization process is controlled by parameters other than global energy conservation within the plasma and that the consideration of process rates must be important.

In view of the observed results, several factors are proposed that may affect the process of particle vaporization, as manifest in the observed upper size limit for complete vaporization. Due to its transient nature, the plasma itself is a nonhomogeneous system in which high-temperature gradients are present; hence, thermophoretic forces could propel the solid particle out of the plasma or to cooler regions, subsequently limiting the vaporization process prior to complete vaporization. Another contributing factor toward incomplete vaporization may be linked to the physical vaporization processes. During the first few nanoseconds of plasma expansion, one side of the particle is subjected to a greater radiant flux and may consequently undergo a faster rate of vaporization. As a result of differing rates of surface evaporation or phase explosion, significant momentum may be transferred to the remaining solid particle, which like thermophoresis may displace the particle to less energetic plasma regions. Finally, vaporization may be limited by the rate of energy transfer (during the first nanoseconds of plasma-particle interaction) from the plasma to the particle. When the heating time is shorter than a

characteristic time of mechanical relaxation, the particle does not have time to expand and heating occurs at nearly constant volume. This constant-volume heating induces a pressure buildup that can fracture and break particles into many smaller pieces,²³ which are readily vaporized within the plasma volume. Such a process favors smaller sized particles characterized by greater surface-to-volume ratios. In summary, most likely the particle vaporization starts within the time scale of the laser pulse and ends within tens of nanoseconds of the laser pulse, before recombination processes become a significant component of the laser-induced plasma evolution. While factors such as thermophoretic forces and vapor expulsion may influence the vaporization dynamics in view of

(23) Zhigilei, L. V.; Garrison, B. J. *Appl. Surf. Sci.* **1998**, 127–129, 142–150.

plasma temperature gradients, additional experimental work and plasma modeling are needed to further determine the exact processes that govern particle vaporization, as well as to determine particle size limits for different laser pulse energies, focusing optics, and particle types.

ACKNOWLEDGMENT

The authors acknowledge Kenjiro Iida for assistance with the alternative data processing algorithm. This research was supported in part by Sandia National Laboratories, Livermore, CA.

Received for review April 23, 2002. Accepted August 22, 2002.

AC020261M